JIRRS
Journal International Review of Research Studies

Received: 02/07/2026 - **Accepted:** 30/08/2026
Vol: 01.09
DOI: 10.66104/swmp0r98
Pages: 1-26

Diagnostic-Leaching Response Fingerprints of Heterogeneous Copper Ores: Mineralogical Context, Copper Accessibility, and Unresolved Deportment

Antonio Clareti Pereira, PhD
PhD in Chemical Engineering
University of São Paulo (USP)
Belo Horizonte, Minas Gerais, Brazil
E-mail: claretipereira@gmail.com
ORCID: https://orcid.org/0000-0001-8115-4279

Abstract

Total copper grade does not necessarily rank the hydrometallurgical response of heterogeneous copper ores because the accessible fraction of Cu depends on mineral association, gangue composition, oxidation state, and the chemical and thermal severity of the leaching environment. This study integrates bulk chemistry, an archived reported modal-mineralogy dataset, dry-residue mass balances, and independent-aliquot diagnostic leaching for four coded copper-ore samples (PQH-CU001 to PQH-CU004). The archive contains no documented within-sample process replication; accordingly, the work is a descriptive, archived-data response-fingerprint reanalysis rather than a statistically validated geometallurgical domain or predictive model. Feed Cu ranged from 0.659 to 1.355 wt%, while the reported mineral assemblages contained strongly variable proportions of biotite (28.90–37.78 wt%), Fe oxyhydroxides (9.13–41.08 wt%), quartz (10.10–23.06 wt%), chlorite (3.82–16.65 wt%), and garnet (6.44–13.56 wt%). Explicitly reported Cu oxyhydroxides represented only 0–0.04 wt% and were quantitatively insufficient to account for the measured bulk Cu grades. Residue-inventory-based apparent Cu extraction ranged from 12.77 to 38.69% in nominal 5% acetic acid, 22.89 to 52.86% in nominal 5% sulfuric acid, and 50.05 to 74.24% under a hot ferric-sulfate condition at approximately 90 °C. The observed accessibility ranking was invariant across all three environments: PQH-CU003 > PQH-CU004 > PQH-CU002 > PQH-CU001. The lowest-grade sample, PQH-CU003 (0.659 wt% Cu), showed the highest fractional extraction, whereas the highest-grade sample, PQH-CU002 (1.355 wt% Cu), was substantially less accessible. On an original-ore basis, Cu remaining after the hot-ferric condition ranged from 0.170 to 0.638 wt%, with PQH-CU001 and PQH-CU002 retaining 0.638 and 0.614 wt% Cu, respectively. Fe-oxyhydroxide abundance alone did not reproduce the extraction ranking, and similar dry-residue yields were associated with widely different Cu extractions. The observations identify an unresolved Cu-deportment gap and diagnostic response fingerprints, but they do not resolve Cu host phases. Because the diagnostic conditions were applied to independent aliquots, and because the hot ferric test also differed in temperature and acidity environment, differences among conditions are operational extraction contrasts rather than sequential mineral fractions or a ferric-specific effect.

Keywords: copper; diagnostic leaching; process mineralogy; ferric sulfate; sulfuric acid; geometallurgy

CC BY

JIRRS
Journal International Review of Research Studies

Received: 02/07/2026 - **Accepted:** 30/08/2026
Vol: 01.09
DOI: 10.66104/swmp0r98
Pages: 1-26

Highlights

- Cu grade did not rank fractional accessibility across the four archived ore samples.
- Reported Cu oxyhydroxides were quantitatively insufficient to explain the measured bulk Cu inventory.
- The hot ferric condition produced the highest extraction, but its increment combines thermal and chemical effects.
- Similar dry-residue yields but widely different Cu extractions indicate selective accessibility rather than bulk dissolution alone.

1. Introduction

Hydrometallurgical processing of oxidized, transitional, and otherwise heterogeneous copper ores is governed by more than the total copper assay. The mineralogical form of Cu, its exposure and grain-scale association, the reactivity of gangue, and solution chemistry collectively determine whether copper is rapidly dissolved, progressively mobilized under more severe conditions, or retained in a less accessible residue. This distinction is central to heap, vat, and agitated leaching because a grade-based classification can group materials with very different acid demand and recovery potential (Chetty, 2018; Petersen, 2016; Thomas, 2021).

Sulfuric acid is the conventional lixiviant for many copper oxide systems, but Cu dissolution depends on acid concentration, particle size, temperature, contact time, and the abundance and reactivity of gangue minerals. Laboratory studies on real oxide ores have shown that increasing acid strength or improving mineral exposure can substantially increase Cu recovery while simultaneously dissolving Fe-, Al-, Mg-, and Ca-bearing gangue (Apua & Madiba, 2021; Kang et al., 2021). Recent work further shows that complex oxide ores may require mineralogy-informed preconcentration or modified leaching routes when conventional direct acid leaching is inefficient (Liang et al., 2024). Consequently, the same bulk Cu grade can produce markedly different metallurgical responses when Cu occurs in different mineralogical or textural settings.

Gangue mineralogy is especially important in altered ores. Biotite, chlorite, kaolinite, and other phyllosilicates can contribute to acid consumption, surface reactions, and secondary precipitation, while Fe-rich phases can host, adsorb, or physically shield finely distributed Cu. Chetty (2018) emphasized that mineral abundance, texture, and reactivity must be considered jointly when

CC BY

JIRRS
Journal International Review of Research Studies

Received: 02/07/2026 - **Accepted:** 30/08/2026
Vol: 01.09
DOI: 10.66104/swmp0r98
Pages: 1-26

predicting leach behavior, and Thomas (2021) identified biotite and chlorite as important contributors to long-term gangue acid consumption. Henne et al. (2021) demonstrated that supergene alteration can structurally incorporate Cu into vermiculite and kaolinite derived from phyllosilicates, with encapsulation by less-altered biotite further restricting accessibility. More recent surface chemistry work also demonstrates that Cu(II) can interact strongly with phyllosilicates via adsorption and ion exchange (Valenzuela-Elgueta et al., 2025).

The importance of direct Cu deportment becomes evident when modal mineralogy nearly closes the bulk-sample mass, yet explicitly identified Cu minerals cannot account for the chemical Cu grade. Modern process mineralogy distinguishes bulk modal abundance from liberation, mineral association, texture, and element-specific deportment; SEM-based quantitative mineralogy and mineral liberation analysis were developed to quantify precisely these relationships rather than infer them from grade alone (Gottlieb et al., 2000; Fandrich et al., 2007; Baum, 2014; Lotter et al., 2018). Process-mineralogy studies of refractory copper ores have shown that substantial Cu can occur in combined forms associated with Fe-rich phases or gangue minerals, producing low acid-leach recovery despite superficially favorable mineral assemblages (Pan et al., 2024; Li et al., 2025). Owen et al. (2024) further showed, at the column scale, that reactive aluminosilicate gangue and secondary silica-rich products can govern Cu accessibility and passivation behavior. Recent work on automated and optical mineralogical characterization also emphasizes the importance of validated sample preparation and mineral-identification workflows when mineral abundance, grain size, liberation, and association are used for geometallurgical interpretation (De Castro et al., 2022; Garner et al., 2024; Koh et al., 2024). These observations caution against equating bulk modal categories with actual element deportment without element-specific validation.

For Cu that responds incompletely to proton-promoted dissolution, ferric iron can provide an additional oxidative pathway. Ferric-assisted dissolution of chalcocite and chalcopyrite depends on Fe^{3+} concentration, redox potential, temperature, surface products, and intermediate Cu–S phases (Fang et al., 2022, 2024; Nyembwe et al., 2024). A hot ferric diagnostic condition can therefore reveal additional apparent Cu accessibility; however, unless temperature and ferric

CC BY

JIRRS
Journal International Review of Research Studies

Received: 02/07/2026 - **Accepted:** 30/08/2026
Vol: 01.09
DOI: 10.66104/swmp0r98
Pages: 1-26

chemistry are independently controlled and residues are characterized, the incremental response cannot be assigned to a unique mineral or to Fe^{3+} alone.

Geometallurgy seeks to integrate mineralogical and metallurgical variability into response domains that predict processing behavior more effectively than grade alone (Barton & North, 2024; Tiu et al., 2023). In the present study, independent-aliquot diagnostic leaching is used only to generate diagnostic response fingerprints. Unlike sequential diagnostic-leaching schemes, the condition-to-condition contrasts reported here cannot be assigned to mineral fractions because separate ore aliquots were tested.

The objective of the present study was to integrate bulk chemistry, an archived reported modal-mineralogy dataset, dry-residue mass balances, and three independent-aliquot diagnostic-leaching environments for four heterogeneous copper-ore samples. The specific aims were to determine whether (i) Cu head grade ranked fractional accessibility; (ii) reported bulk mineralogical attributes covaried with the observed response-fingerprint hierarchy; (iii) the explicitly reported Cu-oxyhydroxide category could account quantitatively for the measured Cu inventory; and (iv) the hot ferric condition produced a substantial additional operational extraction response relative to the unheated acid conditions. The intended contribution is a bounded response-fingerprint interpretation of archived records, not a full process-mineralogical deportment model.

2. Materials and Methods

2.1. Samples, coding, historical classification, and data hierarchy

The available archive for the present reanalysis comprised four copper ore samples, identified throughout this article as PQH-CU001, PQH-CU002, PQH-CU003, and PQH-CU004. The source campaign treated the materials in the context of oxidized copper ore characterization; however, the surviving records do not independently establish the full extent of Cu mineral deportment, and minor residual sulfides cannot be excluded. For this reason, the revised manuscript uses the broader term “heterogeneous copper ores” except when discussing the historical processing context.

CC BY

JIRRS
Journal International Review of Research Studies

Received: 02/07/2026 - **Accepted:** 30/08/2026
Vol: 01.09
DOI: 10.66104/swmp0r98
Pages: 1-26

The study is a quality-controlled reanalysis of an archived bench-scale diagnostic-leaching campaign. Sample coding was used to decouple scientific interpretation from original project identifiers. The surviving records consisted of execution worksheets, analytical workbooks, dry-residue masses, feed assays, residue assays, and a modal-mineralogy table identified in the archive as corrected. Execution worksheets were used to verify reagent preparation and test conditions, while consolidated analytical workbooks were used for Cu mass-balance calculations, in which feed mass, dry-residue mass, feed Cu, and residue Cu were explicitly paired. Conditions lacking an unambiguous mass-assay pairing were excluded from quantitative comparison, and no missing analytical values were estimated. This study prioritizes internally consistent reanalysis of preserved records over retrospective reconstruction of missing experimental detail.

2.2. Bulk chemical composition

Table 1 presents the bulk chemical composition used to characterize the four coded samples. Cu content spans a twofold range, while Fe, Si, Al, Mg, Mn, Ti, K, P, and loss on ignition (LOI) also vary substantially. These contrasts provide the chemical basis for evaluating whether grade or matrix composition better organizes the observed diagnostic response.

Table 1. Bulk chemical composition of the investigated copper-ore samples.

Component	PQH-CU001	PQH-CU002	PQH-CU003	PQH-CU004
Cu (wt%)	1.278	1.355	0.659	0.951
Fe (wt%)	24.903	32.096	36.002	17.332
Si (wt%)	14.709	10.926	14.538	20.743
Al (wt%)	5.385	5.549	3.541	6.380
Mg (wt%)	0.699	0.440	0.601	1.548
Mn (wt%)	1.396	0.639	0.184	0.178
Ti (wt%)	1.397	0.972	0.234	0.313
K (wt%)	1.270	1.736	1.496	1.419
P (wt%)	0.171	0.176	0.063	<0.046
LOI (wt%)	10.306	10.573	4.590	9.279
Zn (mg kg^{-1})	99.2	56.3	28.9	83.6

Source. Consolidated from the archived analytical workbook used in this study. Values below quantification are retained as reported.

CC BY

JIRRS
Journal International Review of Research Studies

Received: 02/07/2026 - **Accepted:** 30/08/2026
Vol: 01.09
DOI: 10.66104/swmp0r98
Pages: 1-26

2.3. Archived reported modal mineralogy and derived assemblages

The archive contained a table identified as "corrected modal mineralogy," but the surviving documentation does not preserve the original pre-correction values, the analytical technique used to generate the modal percentages, or a description of the correction procedure. Consequently, the present study does not independently validate the phase-identification method or the correction history. To avoid implying analytical certainty that cannot be demonstrated, the dataset is referred to here as the archived reported modal mineralogy and is used only as a descriptive bulk-mass dataset.

Table 2 reports the archived modal distribution used for descriptive calculations and interpretations. The reported modal closure ranges from 99.11 to 99.75 wt%, indicating near-complete arithmetic closure of the listed major phases, but closure alone does not validate phase identification or Cu deportment. No technique-specific detection limit, liberation statistic, grain-size distribution, or grain-scale textural relationship is inferred from these data.

Table 2. Archived reported modal mineralogy of the four samples (wt%).

Mineral	PQH-CU001	PQH-CU002	PQH-CU003	PQH-CU004
Quartz	11.05	10.10	11.93	23.06
Feldspars	0.06	0.11	0.13	0.96
Chlorite	10.61	3.82	4.46	16.65
Biotite	28.90	37.78	29.95	29.81
Amphiboles	3.39	1.12	0.52	1.27
Garnet	10.68	6.44	7.99	13.56
Kaolinite	3.58	1.01	0.92	2.63
Cu oxyhydroxides	0.00	0.04	0.01	0.00
Mn oxides	2.79	0.87	0.54	1.90
Fe oxyhydroxides	24.51	38.04	41.08	9.13
Ilmenite	3.35	0.26	2.04	0.38
Other minerals	0.19	0.16	0.18	0.39
Modal sum	99.11	99.75	99.75	99.74

Source. Archived modal-mineralogy dataset supplied for the present reanalysis. The analytical method and historical correction procedure are not preserved in the surviving documentation.

Figure 1 visualizes the reported mineralogical contrasts in Table 2. The map emphasizes the high Fe-oxyhydroxide contents of PQH-CU002 and PQH-CU003, the higher quartz and chlorite contents of PQH-CU004, and the more distributed assemblage of PQH-CU001.

CC BY

JIRRS
Journal International Review of Research Studies

Received: 02/07/2026 - **Accepted:** 30/08/2026
Vol: 01.09
DOI: 10.66104/swmp0r98
Pages: 1-26

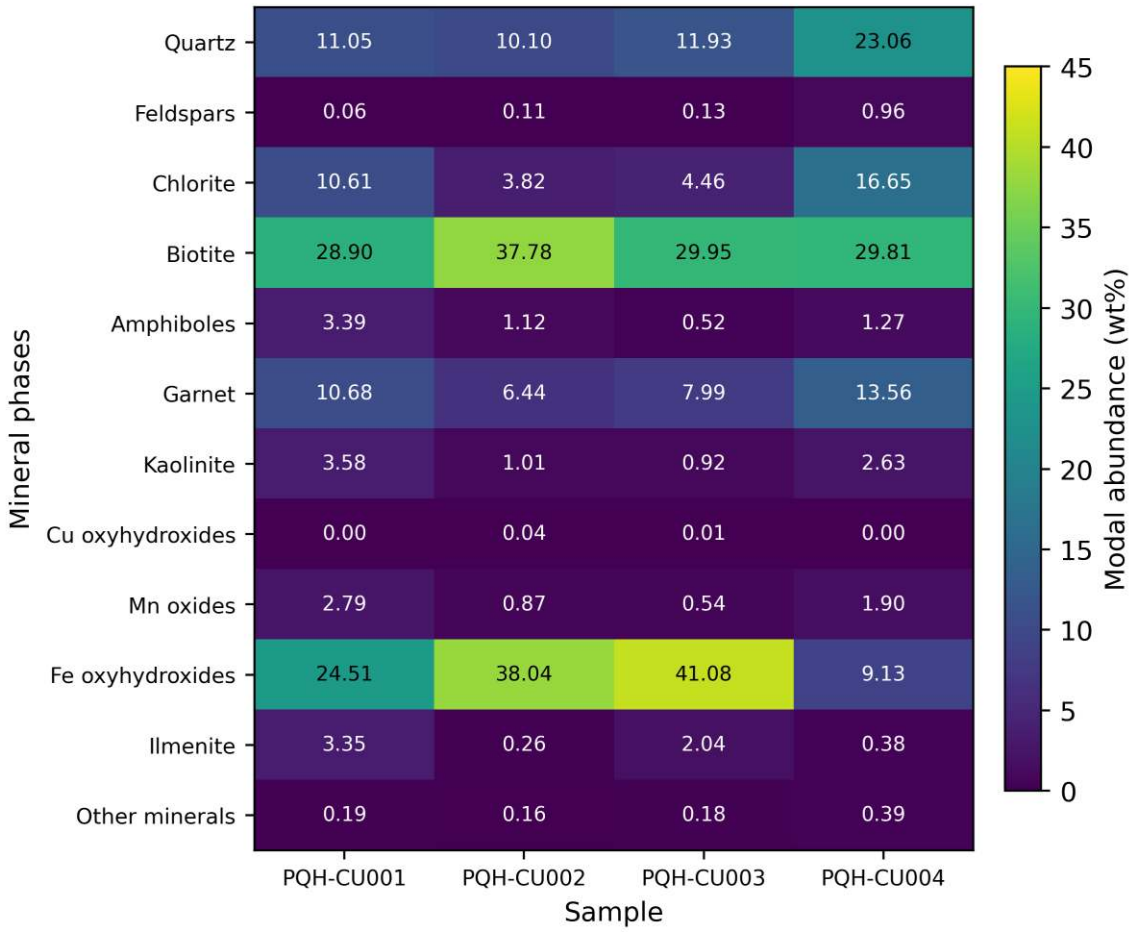

Figure 1. Heat map of the archived reported modal mineralogical distribution of PQH-CU001 to PQH-CU004.

Source. Prepared from the archived modal-mineralogy dataset used in this study. Values are reported modal abundances and may not sum exactly to 100 wt% because of rounding and unclassified minor material.

For the derived interpretation, phyllosilicates were defined as chlorite, biotite, and kaolinite. A broader silicate assemblage was defined as quartz + feldspars + chlorite + biotite + amphiboles + garnet + kaolinite. An operational oxide/oxyhydroxide assemblage was defined as Fe oxyhydroxides + Mn oxides + Cu oxyhydroxides + ilmenite. These groupings are descriptive mass fractions and are not intended as thermodynamic, genetic, or element-deportment classes.

CC BY

JIRRS
Journal International Review of Research Studies

Received: 02/07/2026 - **Accepted:** 30/08/2026
Vol: 01.09
DOI: 10.66104/swmp0r98
Pages: 1-26

2.4. Independent-aliquot (non-sequential) diagnostic-leaching conditions and reproducibility status

Table 3 summarizes the three independent-aliquot leaching environments retained for quantitative comparison. The acetic- and sulfuric-acid tests used approximately 10 g of ore and 500 mL of lixiviant for 60 min, with mechanical agitation at approximately 300 rpm. The hot ferric-sulfate test used the same nominal ore-to-solution scale, a nominal 5% ferric-sulfate solution adjusted to a pH of approximately 1, and a temperature of 89–91 °C for 60 min. After leaching, slurries were filtered, cakes were washed, and residues were dried at approximately 90 °C before chemical analysis. Each environment was applied to a separate ore aliquot; the tests therefore do not constitute a sequential diagnostic-leaching sequence.

Reproducibility status. Preserved variables include approximate ore mass, lixiviant volume, nominal reagent identity and concentration, test duration, approximate agitation for the unheated acid tests, hot-ferric pH and temperature, filtration/washing/drying sequence, paired feed and dry-residue masses, and feed/residue Cu assays used for inventory calculations. Variables unavailable from the surviving archive are the particle-size distribution and sample-preparation protocol; exact mass/volume basis of the nominal 5% reagent concentrations; reagent grades; ferric-sulfate hydration state; pH-adjustment reagent; agitator geometry; exact ambient-test temperature; wash-water volume and detailed protocol; complete analytical-method metadata; and within-sample process replication. These variables cannot be reconstructed defensibly and are not assumed. Consequently, the three conditions are treated as historical diagnostic environments, not as equal-acidity, equal-redox, or fully reproducible mechanistic experiments.

Table 3. Principal diagnostic-leaching conditions retained for Cu mass-balance analysis.

Condition	Ore mass	Lixiviant	Volume	Time	Other conditions
Acetic acid	~10 g	Nominal 5% CH_3COOH	500 mL	60 min	~300 rpm; no external heating recorded
Sulfuric acid	~10 g	Nominal 5% H_2SO_4	500 mL	60 min	~300 rpm; no external heating recorded
Hot ferric sulfate	~10 g	Nominal 5% $Fe_2(SO_4)_3$; pH ~1	500 mL	60 min	Agitated; 89–91 °C

CC BY

JIRRS
Journal International Review of Research Studies

Received: 02/07/2026 - **Accepted:** 30/08/2026
Vol: 01.09
DOI: 10.66104/swmp0r98
Pages: 1-26

Source. Reconstructed from the archived experimental procedure and execution worksheets. The exact concentration basis of the nominal 5% solutions is not preserved.

2.5. Copper mass-balance reconstruction and extraction basis

Copper extraction was reconstructed from the feed and dry-residue inventories rather than inferred solely from solution assays. For each quantified condition, apparent Cu extraction was calculated as:

$$X_{Cu}\ (\%) = 100\ [1 - (m_r\ C_r)/(m_f\ C_f)]$$

where m_f and C_f are the dry feed mass and feed Cu mass fraction, and m_r and C_r are the dry-residue mass and residue Cu mass fraction, respectively. Dry-residue yield was calculated as $Y_r\ (\%) = 100\ m_r/m_f$. Because the present reanalysis does not contain a complete and uniform solution-side mass-balance dataset for all retained conditions, the calculated values are explicitly termed residue-inventory-based apparent extraction. No unsupported solution-plus-residue closure values are introduced.

Because the three lixiviants were applied to independent aliquots rather than sequentially to the same residue, condition-to-condition differences were calculated only as operational contrasts (AcOH denotes acetic acid): $\Delta H_2SO_4–AcOH = XH_2SO_4 - XAcOH$ and the hot-ferric-condition increment relative to $H_2SO_4 = X\text{hot ferric} - XH_2SO_4$. The Cu not extracted under the most severe quantified condition was calculated as 100 − Xhot ferric. These quantities are arithmetic differences between independent diagnostic tests; they are not sequentially isolated Cu fractions and must not be assigned to specific minerals without direct feed-and-residue characterization.

2.6. Small-n descriptive treatment

Only four distinct ore samples were available, with no documented within-sample process replication. Statistical treatment was therefore deliberately descriptive. Observed ranges, rankings, and pairwise contrasts are emphasized. Pearson coefficients were calculated only as exploratory summaries of covariation and are not used for significance testing, prediction, causal attribution, geometallurgical-domain validation, or population-level inference. No p-values, confidence intervals, or regression equations are reported.

CC BY

JIRRS
Journal International Review of Research Studies

Received: 02/07/2026 - **Accepted:** 30/08/2026
Vol: 01.09
DOI: 10.66104/swmp0r98
Pages: 1-26

3. Results

3.1. Mineralogical heterogeneity and the Cu-deportment gap

The samples exhibit sharply different reported mineralogical matrices. Table 4 summarizes derived mineralogical groupings and the quantitative mismatch between the explicitly reported Cu-oxyhydroxide category and the measured chemical Cu grade. PQH-CU004 is the most silicate-rich sample, whereas PQH-CU003 has the highest operational oxide/oxyhydroxide assemblage. PQH-CU002 is dominated by biotite and Fe oxyhydroxides, which together account for 75.82 wt% of the sample.

Table 4. Derived mineralogical descriptors and upper-bound Cu-deportment check.

Sample	Phyllosilicates (wt%)	Silicate assemblage (wt%)	Oxide/ oxyhydroxide assemblage (wt%)	Head Cu (wt%)	Cu oxyhydroxides (wt%)	Maximum bulk Cu explained (%)
PQH-CU001	43.09	68.27	30.65	1.278	0.00	0.00
PQH-CU002	42.61	60.38	39.21	1.355	0.04	≤2.95
PQH-CU003	35.33	55.90	43.67	0.659	0.01	≤1.52
PQH-CU004	49.09	87.94	11.41	0.951	0.00	0.00

Source. Calculated from Tables 1 and 2. The final column is an extreme upper bound obtained by assuming, unrealistically, that the entire reported Cu-oxyhydroxide mass were elemental Cu.

The upper-bound check is deliberately conservative. Even under the physically unrealistic assumption that the entire reported Cu-oxyhydroxide category were pure elemental Cu, it could explain no more than 2.95% of bulk Cu in PQH-CU002 and 1.52% in PQH-CU003. In PQH-CU001 and PQH-CU004, the reported modal abundance of Cu oxyhydroxides is zero despite measurable head grades of 1.278 and 0.951 wt% Cu. Therefore, the overwhelming majority of Cu occurs outside the explicitly reported category of Cu-oxyhydroxide. This establishes a deportment gap but does not identify the unresolved host phases.

CC BY

JIRRS
Journal International Review of Research Studies

Received: 02/07/2026 - **Accepted:** 30/08/2026
Vol: 01.09
DOI: 10.66104/swmp0r98
Pages: 1-26

3.2. Copper extraction and dry-residue yield

Table 5 presents the residue-inventory-based apparent Cu extraction and dry-residue yield for the three quantified diagnostic environments. Extraction increased monotonically from acetic acid to sulfuric acid and then to the hot ferric condition for every sample, but the magnitude of response differed strongly among samples.

Table 5. Apparent Cu extraction and dry-residue yield under the three quantified diagnostic-leaching conditions.

Sample	Acetic Cu extraction (%)	Acetic residue yield (%)	H_2SO_4 Cu extraction (%)	H_2SO_4 residue yield (%)	Hot-ferric Cu extraction (%)	Hot-ferric residue yield (%)
PQH-CU001	12.77	90.62	22.89	86.83	50.05	86.11
PQH-CU002	15.49	88.81	26.04	87.26	54.72	85.71
PQH-CU003	38.69	88.51	52.86	86.08	74.24	86.21
PQH-CU004	20.34	89.18	31.86	86.39	60.61	86.40

Source. Recalculated from paired feed masses, dry-residue masses, feed Cu assays, and residue Cu assays in the archived analytical workbooks. Extraction is residue-inventory-based apparent extraction.

Figure 2 displays the extraction data from Table 5 and makes the invariant sample ranking visually explicit. Across all quantified environments, the observed accessibility order is PQH-CU003 > PQH-CU004 > PQH-CU002 > PQH-CU001.

CC BY

JIRRS
Journal International Review of Research Studies

Received: 02/07/2026 - **Accepted:** 30/08/2026
Vol: 01.09
DOI: 10.66104/swmp0r98
Pages: 1-26

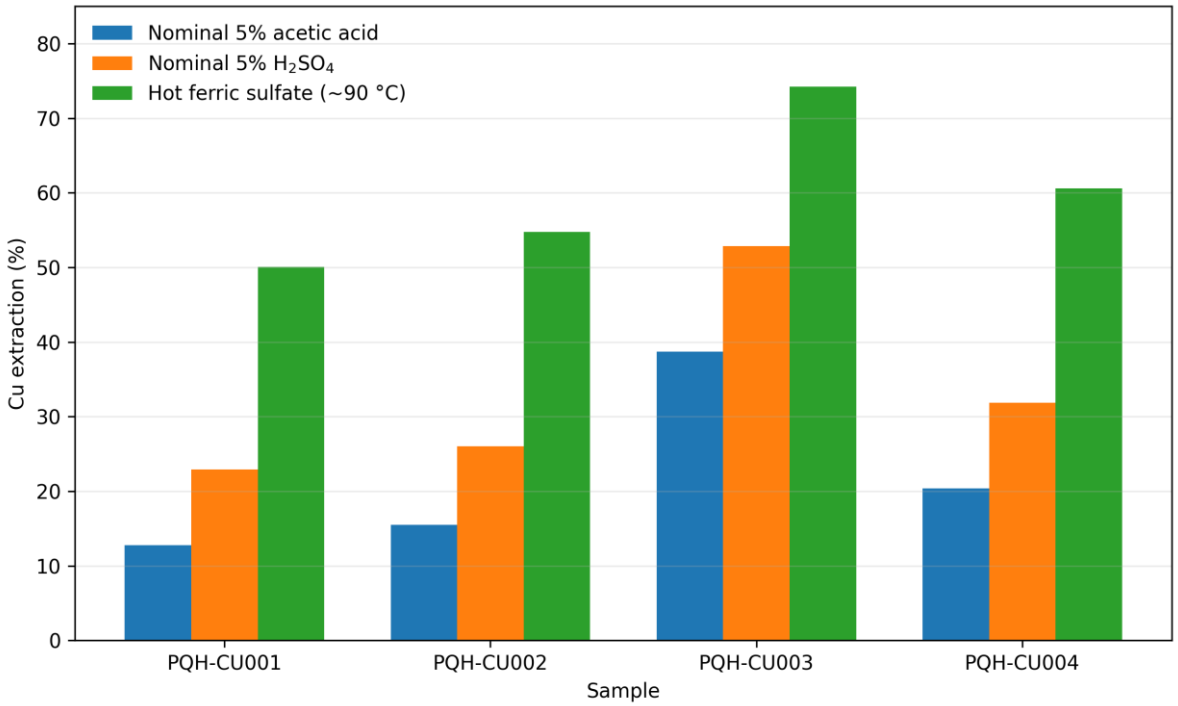

Figure 2. Apparent Cu extraction from PQH-CU001 to PQH-CU004 in nominal 5% acetic acid, nominal 5% sulfuric acid, and the hot ferric-sulfate condition applied to independent ore aliquots.

Source. Prepared from reconstructed archived feed/residue Cu inventories. Each diagnostic condition was applied to an independent ore aliquot; the bars do not represent sequential mineral fractions.

Mean apparent Cu extraction across the four samples increased from 21.82% in acetic acid to 33.41% in sulfuric acid and 59.91% under hot ferric conditions. The sulfuric-acid extraction range was 29.97 percentage points, whereas the corresponding dry-residue-yield range was only 1.18 percentage points. Under hot ferric conditions, apparent Cu extraction spanned 24.19 percentage points while dry-residue yield differed by only 0.69 percentage points. Thus, widely different Cu responses occurred even when gross residual solid mass was nearly the same.

3.3. Observed grade-accessibility inversion

The relationship between Cu head grade and fractional extraction is counterintuitive within this four-sample dataset. PQH-CU003 contains the lowest head grade, 0.659 wt% Cu, yet shows the highest apparent extraction under all three conditions. Conversely, PQH-CU002 contains the

CC BY

JIRRS
Journal International Review of Research Studies

Received: 02/07/2026 - **Accepted:** 30/08/2026
Vol: 01.09
DOI: 10.66104/swmp0r98
Pages: 1-26

highest Cu grade, 1.355 wt%, but ranks only third in fractional accessibility. PQH-CU001, at 1.278 wt% Cu, is the least accessible sample under the tested conditions.

For completeness, descriptive Pearson coefficients between head Cu and apparent extraction are −0.932 for acetic acid, −0.934 for sulfuric acid, and −0.944 for the hot ferric condition. Because n = 4, these coefficients are reported only as compact summaries of the observed ordering and are not treated as inferential or predictive statistics.

Figure 3 shows the four observations under the most severe quantified condition, without a fitted regression line, thereby avoiding a predictive interpretation that is unsupported by the sample size.

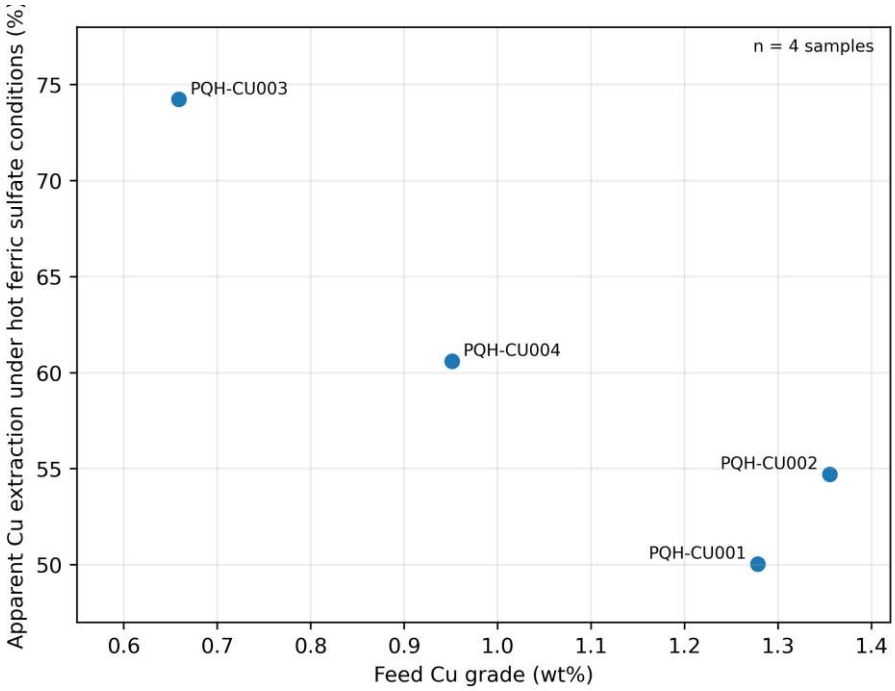

Figure 3. Feed Cu grade versus apparent Cu extraction under the hot ferric-sulfate condition.
Source. Prepared from reconstructed archived feed/residue Cu inventories. Four observations are shown; no regression fit is presented because n = 4 and the relationship is descriptive only.

3.4. Operational extraction contrasts between independent diagnostic conditions

Table 6 reports arithmetic differences between the independent-aliquot diagnostic tests rather than a sequential partition of feed Cu. PQH-CU003 is distinguished by a large weak-acid extraction,

CC BY

JIRRS
Journal International Review of Research Studies

Received: 02/07/2026 - **Accepted:** 30/08/2026
Vol: 01.09
DOI: 10.66104/swmp0r98
Pages: 1-26

whereas PQH-CU001, PQH-CU002, and PQH-CU004 show larger hot-ferric-condition increments relative to unheated sulfuric acid. The final column reports the fraction of feed Cu not extracted under the most severe quantified condition.

Table 6. Operational extraction contrasts and hot-ferric-condition increments calculated from independent diagnostic tests.

Sample	Acetic extraction (%)	H_2SO_4 − AcOH difference (percentage points)	Hot-ferric-condition increment vs H_2SO_4 (percentage points)	Cu not extracted under hot ferric (%)
PQH-CU001	12.77	10.12	27.16	49.95
PQH-CU002	15.49	10.55	28.68	45.28
PQH-CU003	38.69	14.17	21.38	25.76
PQH-CU004	20.34	11.52	28.75	39.39

Source. Calculated from the reconstructed archived inventories reported in Table 5. Differences compare independent ore aliquots and are not sequential mineral-fraction isolations.

Figure 4 presents these contrasts as non-stacked bars to avoid implying that the independent tests constitute a sequential 100% mineralogical partition. The remaining Cu under the hot ferric condition is shown separately from the H_2SO_4-versus-AcOH contrast and the hot-ferric-condition increment relative to H_2SO_4.

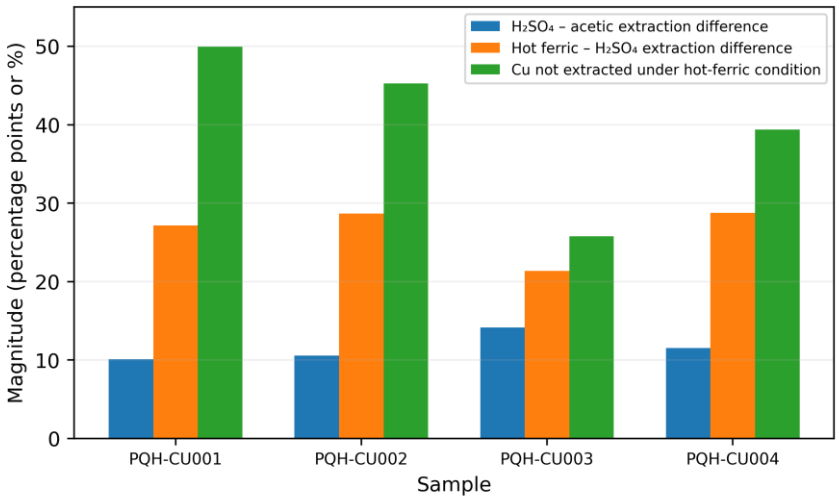

Figure 4. Differential apparent-extraction contrasts between independent diagnostic conditions, including the hot-ferric-condition increment, and Cu not extracted under the hot ferric condition.
Source. Prepared from Table 6 using reconstructed archived feed/residue inventories. The differences are arithmetic contrasts between independent aliquots; they must not be interpreted as mineralogical phase fractions or as uniquely ferric-controlled Cu populations.

CC BY

JIRRS
Journal International Review of Research Studies

Received: 02/07/2026 - **Accepted:** 30/08/2026
Vol: 01.09
DOI: 10.66104/swmp0r98
Pages: 1-26

On an original-ore basis, Cu not extracted under the hot ferric condition is approximately 0.638 wt% Cu in PQH-CU001, 0.614 wt% in PQH-CU002, 0.170 wt% in PQH-CU003, and 0.375 wt% in PQH-CU004. This absolute inventory comparison is process-relevant because the two higher-grade samples retain substantially more Cu in the original ore than the lower-grade, more accessible PQH-CU003. The result reinforces that fractional extraction and absolute unrecovered-metal inventory are distinct descriptors.

3.5. Fe-oxyhydroxide contrast and hypothesis-generating mineralogical associations

A direct internal comparison shows that bulk Fe-oxyhydroxide abundance alone does not reproduce the extraction hierarchy. PQH-CU003 and PQH-CU002 contain similarly high reported Fe-oxyhydroxide contents (41.08 and 38.04 wt%, respectively), yet their hot-ferric apparent extractions differ by 19.52 percentage points (74.24 versus 54.72%). Thus, comparable bulk abundance of the reported Fe-oxyhydroxide category can accompany markedly different Cu accessibility, arguing against a simple interpretation in which Fe-oxyhydroxide abundance itself identifies the dominant Cu host or predicts recovery.

Phyllosilicate abundance shows a different descriptive pattern. The four samples range from 35.33 to 49.09 wt% phyllosilicates, and the hot-ferric-condition increment relative to H_2SO_4 is largest for PQH-CU004, the most phyllosilicate-rich sample. The corresponding exploratory Pearson coefficient is +0.885, but with only four samples, this value is hypothesis-generating only. It is used solely to prioritize future microanalysis of Cu–silicate associations and does not demonstrate that Cu is hosted by phyllosilicates or that phyllosilicate abundance causally produces the observed increment.

4. Discussion

4.1. Grade and accessibility represent different ore attributes

The clearest empirical pattern in this four-sample archived dataset is the persistent inversion between Cu grade and fractional accessibility across the independent-aliquot diagnostic response fingerprints. The lowest-grade sample is the most responsive, whereas the two highest-grade

CC BY

JIRRS
Journal International Review of Research Studies

Received: 02/07/2026 - **Accepted:** 30/08/2026
Vol: 01.09
DOI: 10.66104/swmp0r98
Pages: 1-26

samples retain the largest Cu inventories under the hot ferric condition. This supports a geometallurgical interpretation in which Cu grade and diagnostic accessibility should be treated as separate attributes. Tiu et al. (2023) showed that mineralogical variability can be quantified through geometallurgical domains, while Barton and North (2024) demonstrated the value of process-mineralogical descriptors in complex Cu–Co systems. The present study does not define such domains; it provides a bounded response-fingerprint interpretation showing that head grade alone does not rank the observed diagnostic leach response.

This distinction is operationally important but should not be generalized beyond the present case. A higher-grade material may require greater chemical severity, longer residence time, or a different process route to recover the same fraction of its copper, whereas a lower-grade material may contain a larger readily accessible fraction. These contrasts identify variables that a larger replicated geometallurgical program should capture; they do not support direct scale-up, population-level rules, or predictive ore-domain classification from the present four samples.

4.2. The modal Cu-deportment gap is quantitatively large

Near-complete arithmetic closure of the reported modal table might initially suggest a comprehensive bulk mineral description. The Cu balance demonstrates otherwise. The explicitly reported Cu-oxyhydroxide category is approximately one to two orders of magnitude too small to account for the measured Cu grade. This mismatch is not a rounding effect; it is an elemental-deportment gap between the reported bulk modal classification and the chemical Cu inventory.

Process-mineralogy studies provide plausible analogs. Pan et al. (2024) reported a combined copper oxide ore in which a large fraction of Cu occurred in associated forms, while Li et al. (2025) showed that Cu–gangue interactions can strongly limit acid-leaching efficiency in refractory copper oxide ore. Henne et al. (2021) demonstrated structural incorporation of Cu into altered phyllosilicates and fine-scale encapsulation by biotite. These studies confirm that bulk phase abundance and Cu deportment are not interchangeable measurements.

For the present samples, unresolved Cu could occur as fine- or sub-resolution discrete Cu minerals, Cu structurally incorporated in Fe oxyhydroxides or silicates, Cu adsorbed on reactive mineral

CC BY

JIRRS
Journal International Review of Research Studies

Received: 02/07/2026 - **Accepted:** 30/08/2026
Vol: 01.09
DOI: 10.66104/swmp0r98
Pages: 1-26

surfaces, Cu associated with phyllosilicates by ion exchange or surface complexation, residual sulfides, or other minor phases not separated by the historical modal classification. The current dataset identifies unresolved deportment as the dominant analytical gap but cannot discriminate among these possibilities. Direct grain-scale element mapping and validated Cu-phase identification are required before any of these candidate hosts can be accepted as the controlling mechanism.

4.3. Why Fe-oxyhydroxide abundance alone is not a recovery predictor

PQH-CU003 is both Fe-oxyhydroxide rich and highly accessible, which could tempt a direct host-phase interpretation. PQH-CU002 argues against that simple model: it contains nearly as much reported Fe oxyhydroxide as PQH-CU003 but is much less accessible across all diagnostic environments. The more defensible interpretation is that the nature of Cu association within the Fe-rich matrix may differ among samples. Grain size, porosity, mineral-replacement textures, structural incorporation, surface adsorption, and encapsulation are hypotheses requiring direct element mapping; the present bulk data do not demonstrate Fe oxyhydroxides as Cu hosts.

4.4. Phyllosilicates, gangue reactivity, and the hot-ferric contrast

The phyllosilicate pattern is more nuanced. Phyllosilicate-rich materials need not host the Cu directly; instead, phyllosilicate abundance can act as a proxy for alteration style, acid demand, surface chemistry, and textural association. Chetty (2018) and Thomas (2021) emphasized the reactivity of silicate gangue in copper leaching, while Henne et al. (2021) documented Cu-bearing altered phyllosilicates, and Valenzuela-Elgueta et al. (2025) demonstrated mineral-specific Cu(II) adsorption and ion-exchange interactions on phyllosilicate surfaces. Owen et al. (2024) further showed that aluminosilicate dissolution and the formation of secondary silica-rich phases can materially constrain Cu recovery during column leaching.

PQH-CU004 combines the highest reported phyllosilicate abundance (49.09 wt%) with the largest hot-ferric-condition increment relative to H_2SO_4 (28.75 percentage points). This combination makes PQH-CU004 a priority sample for future grain-scale investigation of Cu–silicate

CC BY

JIRRS
Journal International Review of Research Studies

Received: 02/07/2026 - **Accepted:** 30/08/2026
Vol: 01.09
DOI: 10.66104/swmp0r98
Pages: 1-26

associations, but it is a prioritization hypothesis only and does not establish a causal relationship between phyllosilicate abundance and Cu extraction.

4.5. Interpretation of the hot ferric response

The hot ferric condition yields the highest apparent Cu extraction across all samples. Ferric iron is a well-established oxidant of reduced copper sulfides, and recent studies show that Fe^{3+} concentration, solution potential, temperature, and intermediate Cu–S phases influence the dissolution of chalcocite and chalcopyrite (Fang et al., 2022, 2024; Nyembwe et al., 2024). However, the present historical experiment does not isolate an Fe^{3+} effect because the hot ferric test differs in temperature from the unheated acid tests and does not preserve the exact acidity basis.

Accordingly, the arithmetic increase from the unheated H_2SO_4 test to the hot ferric test is termed the hot-ferric-condition increment. It may include faster proton-promoted dissolution, ferric oxidation, changes in mineral-surface passivation, improved diffusion, or dissolution of phases that are kinetically inaccessible at lower temperature. Because temperature, acidity environment, and ferric oxidation were not independently controlled, assigning this increment to a sulfide fraction or to Fe^{3+} alone would overstate the evidence.

4.6. Similar solid yields but different Cu extraction

The narrow dry-residue-yield range, compared with the broad Cu-extraction range, provides an internal process contrast showing that Cu release is not controlled by gross residual-solid mass alone. Under the hot ferric condition, the four samples retain 85.71–86.40% of their original dry mass, yet apparent Cu extraction ranges from 50.05 to 74.24%. Under sulfuric acid, the residue-yield range is similarly narrow relative to the 29.97-percentage-point extraction range.

Residue yield is not equivalent to gangue dissolution because dissolution and secondary precipitation can occur simultaneously and because different mineral reactions can offset one another in the final dry mass. The residue-yield comparison therefore cannot quantify gangue dissolution. It does show, however, that substantially different Cu release occurred without a

CC BY

JIRRS
Journal International Review of Research Studies

Received: 02/07/2026 - **Accepted:** 30/08/2026
Vol: 01.09
DOI: 10.66104/swmp0r98
Pages: 1-26

proportional difference in total residual mass, supporting selective accessibility as a process-development question rather than gross mass loss as a recovery surrogate.

4.7. Sample-specific geometallurgical profiles

PQH-CU003 is a low-grade but highly accessible sample under the tested conditions. It contains 41.08 wt% reported Fe oxyhydroxides, only 35.33 wt% phyllosilicates, and the largest acetic-acid response. Its Cu inventory, not extracted under hot ferric conditions, is only about 0.170 wt% of the original ore, far below that of the higher-grade samples.

PQH-CU004 is strongly silicate-rich in the reported modal dataset. Its calculated silicate assemblage is 87.94 wt%, its Fe-oxyhydroxide abundance is only 9.13 wt%, and its phyllosilicate content is the highest in the dataset. It exhibits intermediate acid accessibility but a large additional response under the combined hot-ferric condition, making it a useful candidate for future investigation of Cu in altered, silicate-rich material.

PQH-CU002 is a high-grade sample dominated by biotite and Fe oxyhydroxides. Despite the highest Cu head grade, it shows low acetic- and sulfuric-acid extraction and retains approximately 45.28% of its Cu under the hot ferric condition. The behavior demonstrates that abundant Fe oxyhydroxides and a detectable but minor Cu-oxyhydroxide category do not guarantee high Cu accessibility.

PQH-CU001 is the least accessible sample under the tested conditions. It retains the largest absolute Cu inventory under the hot ferric condition, approximately 0.638 wt% Cu in the original ore, and exhibits the lowest extraction under all environments. Its reported assemblage includes substantial biotite, chlorite, Fe oxyhydroxides, garnet, kaolinite, Mn oxides, and ilmenite. These data are consistent with Cu distributed within a complex mineralogical matrix, but the host phases remain unresolved.

4.8. Implications for process development and future ore classification

The results support a response-based characterization strategy in which total grade, validated mineralogical descriptors, element-specific Cu deportment, and independent-aliquot diagnostic

CC BY

JIRRS
Journal International Review of Research Studies

Received: 02/07/2026 - **Accepted:** 30/08/2026
Vol: 01.09
DOI: 10.66104/swmp0r98
Pages: 1-26

accessibility are treated as separate but complementary evidence layers. A future characterization program could combine head Cu, automated or otherwise validated process mineralogy, a mild-acid response, a sulfuric-acid response, and a temperature-controlled oxidizing response before more expensive column or pilot testing. Figure 5 summarizes this logic while explicitly retaining the boundary between measured bulk attributes, unresolved deportment, operational response fingerprints, and process-development implications.

This response-based approach is consistent with previous applications of sequential diagnostic leaching as a supporting tool for the characterization of transitional copper ores (Pereira et al., 2016) and with broader geometallurgical strategies that seek to define process-response domains (Barton & North, 2024; Tiu et al., 2023). The present tests differ from sequential schemes because each condition used an independent ore aliquot. The four-sample dataset therefore cannot define geometallurgical domains or a predictive model; it demonstrates the magnitude and type of contrast that a larger, replicated, mineralogically validated program should capture.

Figure 5 provides a conceptual map of the response-fingerprint interpretation used in this study, showing why head grade, reported modal mineralogy, unresolved Cu deportment, and independent-aliquot accessibility should not be collapsed into a single predictor.

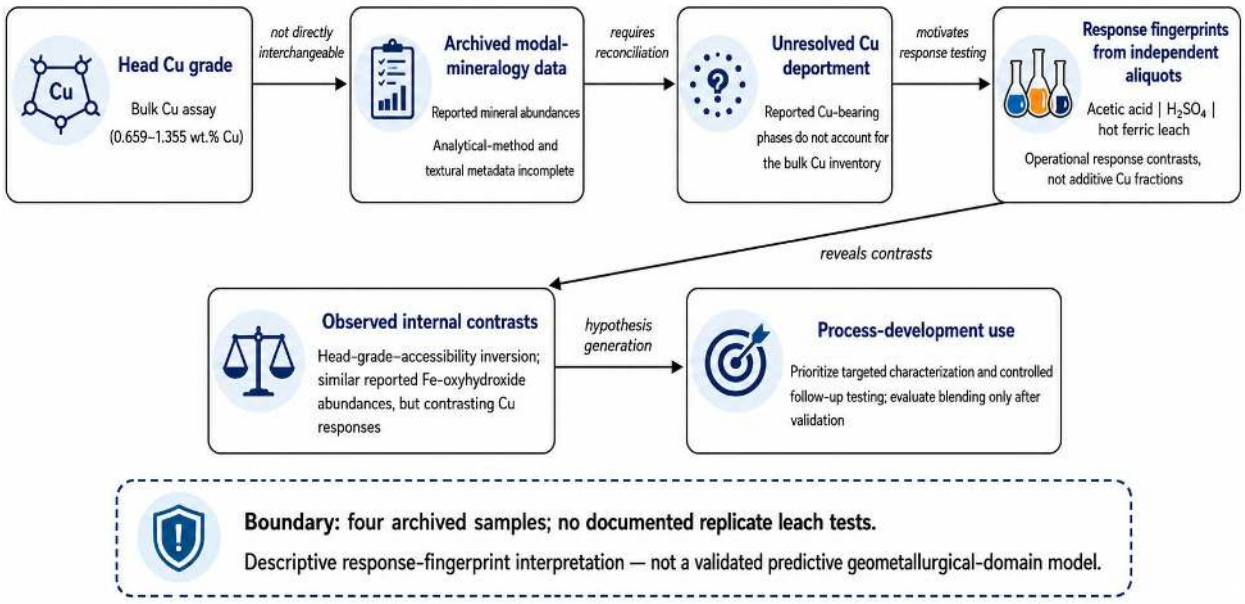

CC BY

JIRRS
Journal International Review of Research Studies

Received: 02/07/2026 - **Accepted:** 30/08/2026
Vol: 01.09
DOI: 10.66104/swmp0r98
Pages: 1-26

Figure 5. Conceptual response-fingerprint framework linking measured bulk descriptors, unresolved Cu deportment, independent-aliquot diagnostic accessibility, and bounded process-development implications.
Source. Conceptual synthesis developed from the present archived-data reanalysis. The framework is descriptive and does not represent a validated predictive geometallurgical model.

4.9. Limitations and research priorities

Sample design and statistical scope. The archive contains four independent ore samples and no documented within-sample process replication. Observed rankings and exploratory correlations are therefore descriptive, do not quantify experimental precision, and cannot establish population-level relationships, predictive rules, or geometallurgical domains.

Mineralogical data and Cu deportment. The historical modal-mineralogy table lacks preserved documentation of the analytical technique, correction procedure, detection limits, liberation statistics, grain size, and texture. Although the reported modal closure is 99.11–99.75 wt%, arithmetic closure does not validate phase identification or element deportment. The present work identifies a large Cu-deportment gap but cannot resolve the actual Cu host phases.

Experimental reproducibility, diagnostic interpretation, and mass-balance closure. Missing experimental metadata include particle-size distribution, sample preparation, exact concentration basis of the nominal 5% solutions, reagent grades, ferric-sulfate hydration state, pH-adjustment reagent, agitator geometry, exact ambient-test temperature, wash-water protocol, and complete analytical-method metadata. The diagnostic tests were performed on independent aliquots rather than sequential residues, so differences among conditions are operational contrasts rather than mineral fractions. The hot ferric test simultaneously changes temperature, acidity environment, and oxidizing chemistry, and therefore does not isolate Fe^{3+}. Finally, a complete and uniform solution-side dataset is unavailable, preventing solution-plus-residue Cu mass-balance closure for all retained conditions.

Future work should prioritize direct Cu deportment in feeds and leach residues using validated automated mineralogy, SEM–EDS or electron-probe element mapping, micro-XRF, and sequential residue characterization (Gottlieb et al., 2000; Fandrich et al., 2007; De Castro et al., 2022; Garner et al., 2024). For the present ore types, a minimum follow-up matrix should separate

CC BY

JIRRS
Journal International Review of Research Studies

Received: 02/07/2026 - **Accepted:** 30/08/2026
Vol: 01.09
DOI: 10.66104/swmp0r98
Pages: 1-26

thermal and ferric effects through four matched conditions: H_2SO_4 at ambient temperature, H_2SO_4 at approximately 90 °C, ferric sulfate at ambient temperature, and ferric sulfate at approximately 90 °C, with acidity basis, solids loading, agitation, and residence time explicitly controlled. Replication, solution Eh and Fe^{2+}/Fe^{3+} measurements where relevant, complete solution-plus-residue Cu closure, and direct mineralogical characterization of each residue would be required before converting the response fingerprints into a mechanistic or predictive process-mineralogy model.

5. Conclusions

Four heterogeneous copper-ore samples with markedly different chemical and reported mineralogical matrices exhibited a systematic hierarchy of Cu accessibility across three historical independent-aliquot diagnostic-leaching environments. Residue-inventory-based apparent Cu extraction increased from 12.77–38.69% in acetic acid to 22.89–52.86% in sulfuric acid and 50.05–74.24% under the hot ferric condition, while the response ranking remained PQH-CU003 > PQH-CU004 > PQH-CU002 > PQH-CU001. Within this bounded four-sample dataset, the lowest-grade sample was the most fractionally accessible, whereas the higher-grade samples retained the largest absolute Cu inventories under the most severe quantified condition. These results demonstrate a grade-accessibility inversion in the archived case, not a population-level predictive relationship.

The archived reported modal mineralogy achieved 99.11–99.75 wt% arithmetic closure, but explicitly reported Cu oxyhydroxides represented only 0–0.04 wt% and could not quantitatively account for the measured chemical Cu grades. The study therefore identifies unresolved Cu deportment as the dominant mineralogical interpretation, but it does not demonstrate whether the missing Cu resides in fine discrete phases, Fe oxyhydroxides, phyllosilicates, adsorbed surface species, residual sulfides, or other minor phases. Fe-oxyhydroxide abundance alone did not reproduce the extraction hierarchy, and similar dry-residue yields accompanied widely different Cu extractions; neither observation is sufficient to assign a specific Cu host without direct grain-scale mapping.

CC BY

JIRRS
Journal International Review of Research Studies

Received: 02/07/2026 - **Accepted:** 30/08/2026
Vol: 01.09
DOI: 10.66104/swmp0r98
Pages: 1-26

Because the tests were performed on independent aliquots and the hot ferric condition also differed in temperature and acidity environment, condition-to-condition differences are operational response contrasts, not sequential mineral fractions or ferric-specific effects. The contribution of this study is therefore a descriptive response-fingerprint interpretation of preserved archived records. Direct Cu deportment, replicated testing, controlled separation of thermal and ferric effects, and complete mass-balance closure are required before broader geometallurgical domains, mechanistic pathways, or predictive rules can be proposed.

Declarations

Competing interests. The authors declare no known competing financial interests or personal relationships that could have influenced the work reported in this article.

Funding. Funding information for the original experimental campaign is not established by the surviving dataset. No additional experimental campaign was conducted for the present reanalysis.

Data availability. The numerical data supporting the reported comparisons are presented in the tables and figures of this article. The study is based on archived laboratory records, analytical workbooks, and an archived modal-mineralogy dataset. Availability of the original source records to third parties is subject to the conditions governing those records.

Ethics statement. Not applicable. The study did not involve human participants, animals, or biological experimentation requiring ethical approval.

References

Apua, M. C., & Madiba, M. S. (2021). Leaching kinetics and predictive models for element extraction from copper oxide ore in sulphuric acid. Journal of the Taiwan Institute of Chemical Engineers, 121, 313–320. https://doi.org/10.1016/j.jtice.2021.04.005

Barton, I. F., & North, R. M. (2024). Geometallurgy of the Tenke-Fungurume sediment-hosted copper-cobalt district, D.R. Congo. Minerals Engineering, 218, 108993. https://doi.org/10.1016/j.mineng.2024.108993

CC BY

JIRRS
Journal International Review of Research Studies

Received: 02/07/2026 - **Accepted:** 30/08/2026
Vol: 01.09
DOI: 10.66104/swmp0r98
Pages: 1-26

Baum, W. (2014). Ore characterization, process mineralogy and lab automation—A roadmap for future mining. Minerals Engineering, 60, 69–73. https://doi.org/10.1016/j.mineng.2013.11.008

Chetty, D. (2018). Acid-gangue interactions in heap leach operations: A review of the role of mineralogy for predicting ore behavior. Minerals, 8(2), 47. https://doi.org/10.3390/min8020047

De Castro, B., Benzaazoua, M., Chopard, A., & Plante, B. (2022). Automated mineralogical characterization using optical microscopy: Review and recommendations. Minerals Engineering, 189, 107896. https://doi.org/10.1016/j.mineng.2022.107896

Fandrich, R., Gu, Y., Burrows, D., & Moeller, K. (2007). Modern SEM-based mineral liberation analysis. International Journal of Mineral Processing, 84(1–4), 310–320. https://doi.org/10.1016/j.minpro.2006.07.018

Fang, C., Cai, T., Yu, S., Gao, L., Huang, L., Peng, H., Qiu, G., & Wang, J. (2022). How ferric salt enhances the first-stage acidic leaching of chalcocite: Performance of intermediate crystallite. JOM, 74(5), 1969–1977. https://doi.org/10.1007/s11837-022-05171-w

Fang, C.-J., Wang, J., & Qiu, G.-Z. (2024). Advancements on chemical-biological dissolution mechanism and leaching kinetics of chalcocite. Transactions of Nonferrous Metals Society of China, 34(1), 283–297. https://doi.org/10.1016/S1003-6326(23)66398-8

Garner, C., Strongman, J., Staniforth, B., Fletcher, J., & Brough, C. (2024). The importance of sample preparation techniques for use in mine site operational mineralogy. Minerals Engineering, 205, 108463. https://doi.org/10.1016/j.mineng.2023.108463

Gottlieb, P., Wilkie, G., Sutherland, D., Ho-Tun, E., Suthers, S., Perera, K., Jenkins, B., Spencer, S., Butcher, A., & Rayner, J. (2000). Using quantitative electron microscopy for process mineralogy applications. JOM, 52(4), 24–25. https://doi.org/10.1007/s11837-000-0126-9

CC BY

JIRRS
Journal International Review of Research Studies

Received: 02/07/2026 - **Accepted:** 30/08/2026
Vol: 01.09
DOI: 10.66104/swmp0r98
Pages: 1-26

Henne, A., Craw, D., Paterson, D., & Southam, G. (2021). Textures and mineralogy of residual supergene copper silicates in oxidized overburden. Minerals Engineering, 163, 106775. https://doi.org/10.1016/j.mineng.2021.106775

Kang, C.-U., Ji, S.-E., Pabst, T., Choi, K.-W., Khan, M. A., Kumar, R., Krishnaiah, P., Han, Y., Jeon, B.-H., & Kim, D.-H. (2021). Copper extraction from oxide ore of Almalyk Mine by H_2SO_4 in simulated heap leaching: Effect of particle size and acid concentration. Minerals, 11(9), 1020. https://doi.org/10.3390/min11091020

Koh, E. J. Y., Amini, E., Spier, C. A., McLachlan, G. J., Xie, W., & Beaton, N. (2024). A mineralogy characterization technique for copper ore in flotation pulp using deep learning machine vision with optical microscopy. Minerals Engineering, 205, 108481. https://doi.org/10.1016/j.mineng.2023.108481

Li, Y., Fu, Y., Kou, J., Liu, Y., Yin, J., Wang, P., & Sun, C. (2025). Acid and impurities-reducing leaching of Muliashi refractory copper oxide ore by stepwise acid addition-starvation leaching: Behavior, mechanism and industrial application. Separation and Purification Technology, 379, 135026. https://doi.org/10.1016/j.seppur.2025.135026

Liang, Z., Wang, Q., Tang, L., Duan, H., Chen, L., Xue, Z., & Li, Y. (2024). Recovery of Cu from copper oxide ore using magnetic separation-leaching process and magnetism study of copper-containing minerals. Minerals Engineering, 218, 109006. https://doi.org/10.1016/j.mineng.2024.109006

Lotter, N. O., Baum, W., Reeves, S., Arrué, C., & Bradshaw, D. J. (2018). The business value of best practice process mineralogy. Minerals Engineering, 116, 226–238. https://doi.org/10.1016/j.mineng.2017.05.008

Nyembwe, K. J., Fosso-Kankeu, E., Waanders, F., Mamba, B. B., & Mkandawire, M. (2024). Chalcopyrite leaching in ferric sulfate: The effect of Fe_3O_4-$CuFeS_2$ galvanic couple on the Cu dissolution. Minerals, 14(2), 162. https://doi.org/10.3390/min14020162

CC BY

JIRRS
Journal International Review of Research Studies

Received: 02/07/2026 - **Accepted:** 30/08/2026
Vol: 01.09
DOI: 10.66104/swmp0r98
Pages: 1-26

Owen, N. D., Ram, R., Vollert, L., Seaman, B., Etschmann, B., Xing, Y., Rosemann, M., Verdugo, L., O'Callaghan, J., & Brugger, J. (2024). The deleterious role of gangue mineralogy in copper extraction: A case study of poor recovery in leaching low-grade Cu ores. Applied Geochemistry, 166, 105984. https://doi.org/10.1016/j.apgeochem.2024.105984

Pan, Z., Jian, C., Peng, Z., Fu, X., He, R., Yue, T., & Sun, W. (2024). Study on process mineralogy of the combined copper oxide ore in Tibet and acid leaching behavior with calcium fluoride. Minerals, 14(4), 352. https://doi.org/10.3390/min14040352

Pereira, A. C., Heck, N. B., & Gomes, M. R. dos S. (2016). Aplicação de diagnóstico de lixiviação como suporte à pesquisa mineral de minério de transição de cobre [Diagnostic leaching application in support of mineral research on transition copper ore]. Tecnologia em Metalurgia, Materiais e Mineração, 13(3), 242–247. https://doi.org/10.4322/2176-1523.0985

Petersen, J. (2016). Heap leaching as a key technology for the recovery of value from low-grade ores: A brief overview. Hydrometallurgy, 165, 206–212. https://doi.org/10.1016/j.hydromet.2015.09.001

Thomas, M. J. (2021). Understanding gangue acid consumption in copper sulfide heap leaching: Predicting the impact of carbonates, silicates and secondary precipitates. Minerals Engineering, 171, 107090. https://doi.org/10.1016/j.mineng.2021.107090

Tiu, G., Ghorbani, Y., Jansson, N., Wanhainen, C., & Bolin, N.-J. (2023). Quantifying the variability of a complex ore using geometallurgical domains. Minerals Engineering, 203, 108323. https://doi.org/10.1016/j.mineng.2023.108323

Valenzuela-Elgueta, J., Delgado, A. V., & Ahualli, S. (2025). Fundamentals of copper(II) adsorption on phyllosilicate minerals relevant to crud formation in solvent extraction from heap leach liquors. Hydrometallurgy, 231, 106409. https://doi.org/10.1016/j.hydromet.2024.106409

CC BY